Arab J. Nucl. Sci. Appl., Vol. 55, 2, 53 -59 (2022)

ISSN 1110-0451

Arab Journal of Nuclear Sciences and Applications

Web site: ajnsa.journals.ekb.eg

(E S N S A)

Synthesis and Characterization of Mn-Doped ZnO Nanoparticles and Effect of Gamma Radiation

Saleh M Abdou*[1] and K M Al-mokhtar[2]

[(1)]*Radiation Physics Department, National Center for Radiation Research and Technology(NCRRT), Atomic Energy Authority, Cairo, Egypt.*

[(2)]*Physics Department, Faculty of Science, Taibah University, Saudia Arabia.*

ARTICLE INFO

Article history:

Received: 30th July 2021

Accepted: 29th Dec. 2021

Keywords:

XRD; PL; UV-VIS; optical properties; Mn-doped ZnO; Co-precipitation; Nanoparticles.

ABSTRACT

Because of their exceptional properties, Mn-doped ZnO nanocrystals are attracting much attention as a semiconductor nanomaterial. Undoped and four levels (1%, 2%, 3% and 4%) of manganese-doped Zinc Oxide were synthesized using co-precipitation procedure. Mn-doped ZnO was characterized using XRD, photoluminescence spectrometer (PL), and optical band gap energy (Eg) measured by UV-visible spectrophotometer. The results showed that no signature of impurity peaks appeared in the XRD pattern of the samples that elucidate Mn attached secondary phases. The 4% manganese-doped Zinc Oxide has the lowest particle size. The optical energy band gap was found to be 2.85 eV for undoped ZnO samples, 2.5 eV for 1% Mn-doped samples and 2.1 eV for 4% manganese-doped Zinc Oxide. The results showed a decrease in the optical band gap through rising Mn concentration, this might be attributed to many discussed reasons. However, there is no change within the magnitude of the optical band gap for the Zinc Oxide and Mn-doped ZnO samples after irradiation with gamma rays at a dose of 30 kGy. The intensity of the PL peak of Mn-doped ZnO showed a decrease after irradiation with gamma raysdose of 30 kGy. The decrease in the PL intensity refers to the reduction of oxygen vacancies due to the indigent interface between ZnO/Mn. In the photoluminescence spectra, ultraviolet emission was recorded for the doped and undoped samples at a wavelength of 368 and 471 nm, respectively and other smaller peak emissions. Thus, Mn-doped ZnO nanoparticles can be used as dilute magnetic semiconductors.

1. INTRODUCTION

Zinc oxide (ZnO) has a high excitation binding energy. It is a necessary semiconductor, because of its potential application in various areas including photo-catalysts, chemical sensors, solar cells and optoelectronic devices. Thus, it has attracted the attention in the area of scientific research and practical purposes. In addition, Zinc Oxide is environmentally friendly and it is of a low cost in comparison with other metal oxides [1]. Because of its high surface area to mass ratio, ZnO nanoparticles may improve the adsorption of organic pollutants [2].

Light absorption catalytic activity is limited for the undoped ZnO nanoparticles. Moreover, ZnO enables absorbing light during UV range only, since it has a large band gap energy. The fast recombination rate of photo-generated electron hole pairs also will share in the determination of photo-catalytic performance [3].

The transition metal-doped ZnO nanoparticles are favored in order to improve electrical, magnetic and optical characteristics of ZnO. The improvement of ZnO nanoparticles with doping material has more applications in spin electronics and UV optoelectronic [4].

The expression "doped" is utilized to improve the magnetic and/or optical characteristics of the host material during supplementing impurity ions in the host lattice. With 3-d metals doping for example, Mn, Cr, Fe, Co and Ni shall reduce the particle size and increase the surface area of ZnO nanoparticles [5].

Corresponding author: salehabdou03@yahoo.com

DOI: 10.21608/ajnsa.2021.88334.1494

A modification of the luminescence pattern, beside, a tenfold decrease in intensity of luminescence was observed, at a doping rate of 1% Mn in the ZnO lattice. Moreover, a reduction of only 30% in the luminescence intensity has occurred as a result of the increase of the dopant percentage from 1% to 5%. The increase percentage of Mn leads to a better photocatalytic activity [6].

Mn-doped ZnO nanoparticles are synthesized in various values of 1%, 2% and 3% through the sol-gel method. All samples are presented in polycrystalline nature, having wurtzite lattice structure with a single phase. The UV-Vis spectra of the nanoparticles show a decline in the band gap energy of 3.08 eV for 1 % Mn-doped to 3.05 eV for 2 % Mn-doped. However, for 3 % doping, it increases to 3.11 eV. The results show the lattice strain related to Mn concentration [7].

Mn-doped ZnO nanocrystals were synthesized through the one-step aqueous solution procedure. As indicated via the PL-spectra, ultraviolet emission has been observed at a wavelength of 389 and 384 nm for the Mn-doped ZnO and ZnO [8].

In the current work, Mn doped ZnO nanoparticles are synthesized with various values of 1%, 2%, 3% and 4% (by weight) through the precipitation procedure, and elaborated their structure, spectroscopy and optical properties. The objective of the current work is to discuss and evaluate the influence of Mn doping on the ZnO Structure, its optoelectronic properties, the spectroscopic analyses of the photoluminescence peak intensity and the effect of gamma irradiation.

2. MATERIALS AND METHODS:

Mn $(OAc)_2 \cdot 4H_2O$ (99.99%,Sigma) and Zn $(OAc)_2 \cdot 2H_2O$ (98%, Sigma) were used, and other required chemicals were of reagent grade. All solutions were produced using Milli-Q water as solvent. Following a Co-precipitation procedure, Mn-doped ZnO nanoparticles were synthesized [3].

The powder samples were irradiated at 30 kGy free in air using GC4000A Cobalt-60 Indian Gamma cell at 0.971 kGy/h dose rate. For structural characterization, XRD analysis of the undoped and Mn-doped Zinc Oxide nanoparticles were carried out using a XRD-6000 Shimadzu Diffractometer.

Perkin Elmer λ35 UV-VIS spectrophotometer was used to achieve the optical absorption spectra. The sample was run in the wavelength range from 800 to 250 nm using spectral bandwidth (SBW) 2 nm with data interval of 1 nm. The spectra were registered in wavelength vs absorbance plots. The Lumina photoluminescence is used in the present analyses at 323 nm excitation wavelength. The applied wavelength Range is 190 - 900 nm for excitation and emission. The peak to peak is better than 1000: 1 and the RMS is better than 4000: 1. The scan speed and the PMT Voltage are 1000 nm/min and 700 V respectively.

3. RESULTS AND DISCUSSION

The structure, spectroscopy and optical properties have been elaborated for characterization of zinc oxide and synthesized manganese doped zinc oxide nanoparticles.

3.1. Structural analysis

For ZnO and the distinct content of Mn -doped ZnO nanoparticles, phase purity and structure parameters were assessed using XRD. The XRD-patterns of ZnO and Mn -doped ZnO nanoparticles in different sample concentration percentages of 1%, 2%, 3% and 4% as presented in Fig. (1).

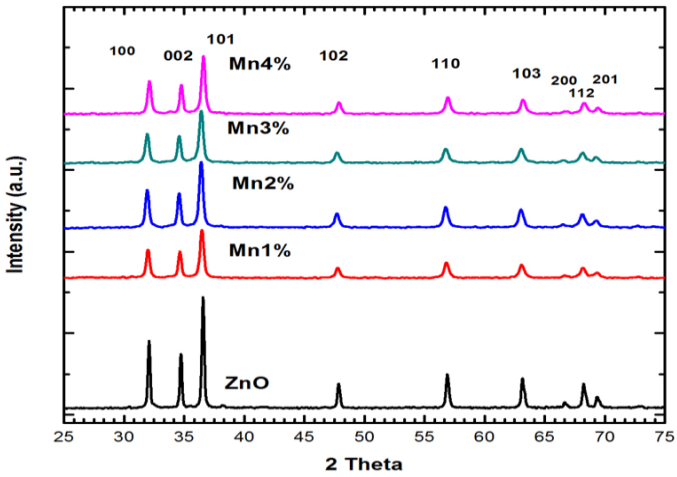

Fig. (1): XRD-patterns of the undoped ZnO (a), and (b) 1 %, (c) 2 %, (d) 3 %, (e) 4 % Mn doped ZnO after the treatment

The intensity of the diffraction peaks corresponds to the hkl planes marked that all sintered samples have a hexagonal (wurtzite) crystal structure. The peak diffraction results presented in Figure (1) are similar to those of the data in the standard powder diffraction file (00-079-0207) of the ZnO phase at (hkl) associated with their peak positions of 2θ as listeed in Table (1).

It is obvious in Fig. (1) that the enhancement in the XRD peak broadening is parallel with increasing Mn content up to 4%. There are no impurity phases, manganese metal or extra peak of oxides and impurity peaks. This means that all samples are single phase [9]. The XRD pattern represents the peaks belonging to wurtzite crystal structure of ZnO only.

Table (1): List of the Miller indices (hkl) to identify the different planes of atoms and the corresponding peak position at (2θ)

hkl	100	002	101	102	110	103	200	112	201
2θ	32.8	34.74	36.56	47.82	56.84	63.14	66.58	68.22	69.36

Without the formation of secondary phases, the Mn ions were directed to the Zn site up to 4% and no change in the crystalline structure after the samples prepared by co-precipitation method. In the Mn-doped ZnO diffraction patterns, the peaks stay at the same 2θ or slightly shifted to a lower angle as contrasted with ZnO nanoparticles. It reveals that the $Mn2^{+}$ ions were directed towards $Zn2^{+}$ sites.

Lattice Parameters. The lattice parameters are specified utilizing the following formula [9]:

$$\frac{1}{d_{hkl}^2} = \frac{4}{3}\left[\frac{h^2 + hk + k^2}{a^2}\right] + \frac{l^2}{c^2} \qquad (1)$$

Where, a & c are the lattice parameters, hkl are the Miller indices and d is the interplanar spacing. The determined data of lattice parameters are reported in Table (2). The lattice parameters increases with rising Mn concentration of the Mn-doped ZnO for the reason that the high ionic radius of the Mn^{2+} ions is compared to the Zn^{2+} ions. Therefore, the lattice parameters rise with a Mn increase up to 4% in ZnO nanocrystals.

Crystallite Size. Based on the Debye–Scherrer formula, the average crystallite size was calculated from the peak width of (101) in the XRD pattern (Fig. 1). The crystallite average size of the samples is determined using the following formula [9] and the calculated results are listed in Table (2).

$$D = K\lambda / \beta_{hkl} \cos\theta \qquad (2)$$

Where D is the crystallite average size in nanometers, β_{hkl} is the peak width at half maximum intensity, the X-ray wavelength λ is 1.54056 A^0 with CuKα radiation and K is a constant equal to 0.9. The crystallite average size was in the domain of 43-83 nm. It might be the doping of Mn in ZnO is able to control crystal size, as noticed for different metals such as Co [10], Cr [11]. It decreases with the rise in the Mn percentage concentrations.

Volume of unit cell

The unit cell volume is obtained utilizing the following formula:

$$V = a2\ c\ (\sqrt{3})/2 \qquad (3)$$

The results indicate that the rise in Mn concentration leads to the unit cell volume increase, which might be attributed to the increase in the lattice parameters. The determined values of the unit cell are recorded in Table (2).

Atomic packing fraction (APF)

APF was obtained utilizing the lattice parameters a & c in the following formula:

$$APF = 2\pi a / 3c\sqrt{3} \qquad (4)$$

The APF calculated values is recorded in the Table (2). With the rise in the Mn concentration, the APF increases, which puts the emphasis on the homogenous substitution of Mn ions in the Zn site of ZnO structure. In addition, this may be due to the decrement of voids in the samples.

Table (2): The lattice parameters, crystallite size (D), volume of unit cell and APF of Mn doped ZnO

Column1	A	C	D	V	APF
ZnO	3.22118686	5.16418	82.95144	46.4049	1.713141
1%	3.23053993	5.17734	51.53384	46.79372	1.71593
2%	3.236452	5.18618	50.02193	47.04533	1.717604
3%	3.23657902	5.18566	48.03566	47.04431	1.717758
4%	3.21856569	5.15992	43.32159	46.29119	1.712453

3.2. Optical Properties

The data obtained, on the optical absorbance of the undoped and Mn-doped ZnO samples, were performed in the wavelength range of 200–1100nm. The UV–Vis spectra at various doping levels are 1%, 2%, 3% and

4% of manganese-doped Zinc Oxide. Whereas, the Mn level percentage is raised, the intensity reduced as presented in Fig. (2).

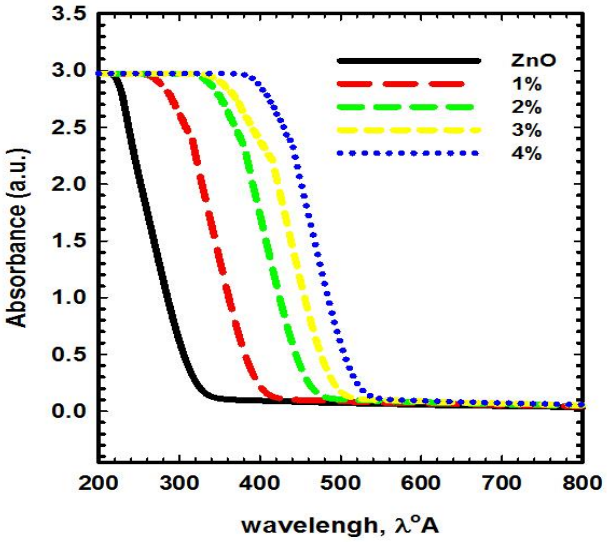

Fig. (2): Displays the spectra of the UV–VIS at doping levels of 1%, 2%, 3% and 4%

From the absorption spectra (Fig. 2), the absorption coefficient α is determined using the following formula:

$$\alpha = -(1/d)\,A \qquad (5)$$

Whereas A is the absorbance and d is the sample cell thickness = 1 cm. The relationship between hν the incident photon energy and α the absorption coefficients in the high absorption region is formed [9]:

$$\alpha h\nu = C\,(h\nu - Eg)^n \qquad (6)$$

Where C is a constant, Eg is the energy band gap of the material, and n defines the manner of the optical transition. Where, indirect and allowed transition n = 2, direct transition n = 1/2 and for direct forbidden n = 3/2. ZnO is a direct bandgap semiconductor. So, utilizing the Tauc's relation is used to determine the bandgap energy of the samples that includes the plot of the graph in Fig. (3) which illustrates a relation $(\alpha h\nu)^2$ vs. hν.

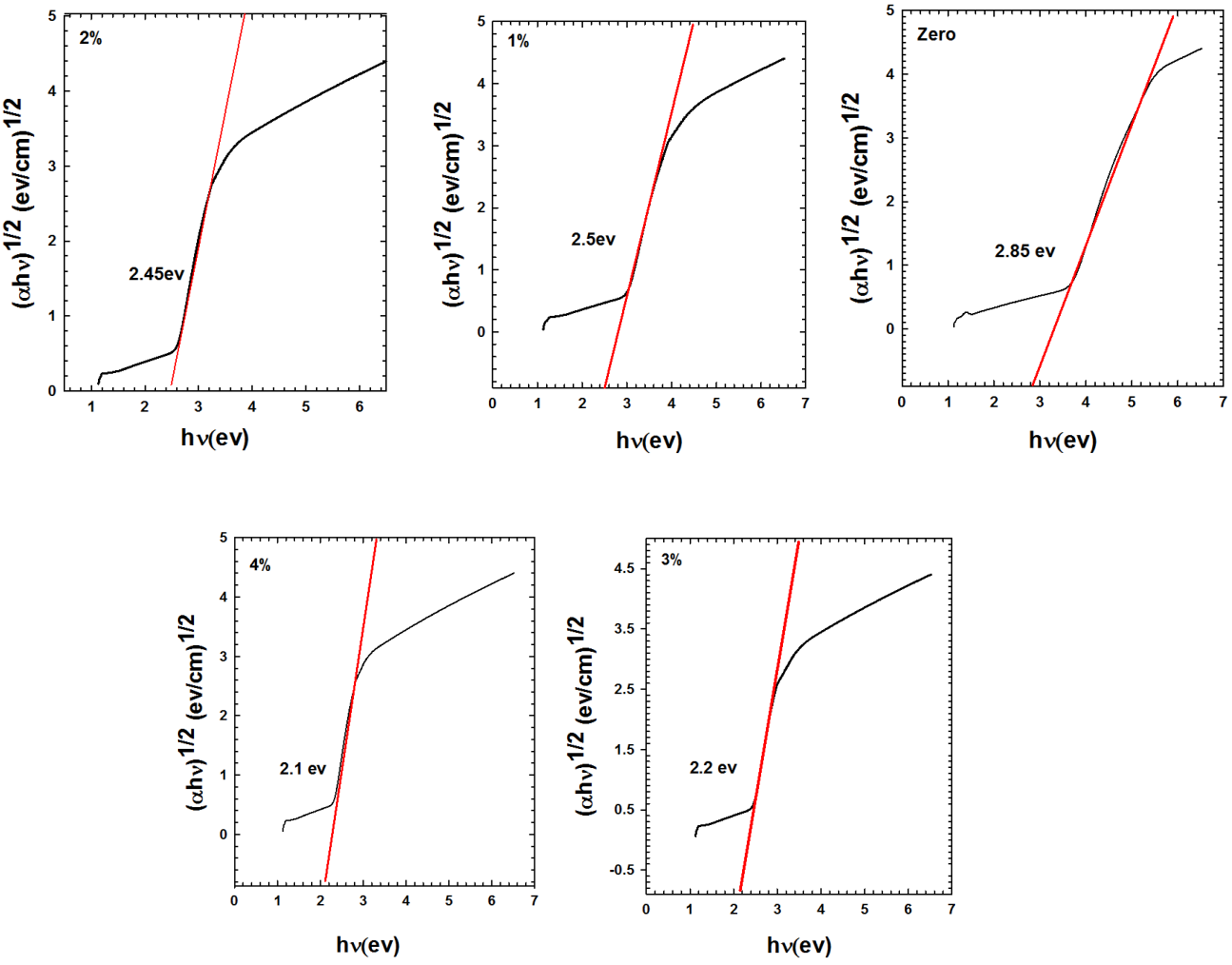

Fig. (3): Tauc's relation of $(\alpha h\nu)^2$ vs. hν to determine the band gap energy of the samples at different doped Mn percentages

The intercept of the linear section of the curve (αhν)2 at Y=0 is equal to the band gap energy (Eg). The doping level as displayed in Fig. (3), it was raised from 0 to 4 %, Eg decreased from 2.85 to 2.1 eV. This may be attributed to the impact of many agents for example carrier concentrations, structural parameters, and the appearance of defects including oxygen vacancies [13]. Moreover, the distinguished reduction in Eg with the increase in Mn content might be because of the spin exchange interaction between localized spins of the Mn ions in the forbidden band and the sp band [14]. Lastly, an increment of surface area to volume ratio might be expected to Mn cluster, and a decrease in crystallite size average [12].

The gamma irradiation effect on Eg was studied by many authors [12,15,16] for ZnO and Mn-doped ZnO nanoparticles. It is found that after irradiation at a dose of 30 kGy, no change was observed in Eg of ZnO samples [17]. The high radiation resistance and poor sensitivity to ionizing radiation may be due to its composition nature and the high consistent energy.

3.3. Photoluminescence (PL)

Photoluminescence(PL) is a form of electromagnetic spectroscopy that analyses the fluorescence of the sample. The PL analyses of the undoped ZnO and 1%, 2%, 3% and 4% manganese doped zinc oxide where performed using a Lumina fluorescence spectrometer. The PL spectra of undoped ZnO and Mn-doped ZnO at 1% and 4% are displayed in Fig. (4). It is clear that, the intensity decreased as the doping level increased.

At the broadband gap of zinc oxide, the violet emission relative with the near band edge emission under 323 nm excitation wavelength, is attributed to the annihilation of exciton. As observed in the photoluminescence spectra, ultraviolet emission is recorded at ZnO and ZnO doped Mn nanoparticles for wavelengths of 468 and 471 nm respectively. It may be related to the exciton transitions and other smaller emissions.

The shift in the PL emission peak (3 nm) between the doped and undoped nanocrystals relates to the modification in Eg. In addition, the deep level emissioncorresponds to the structural defects [18].

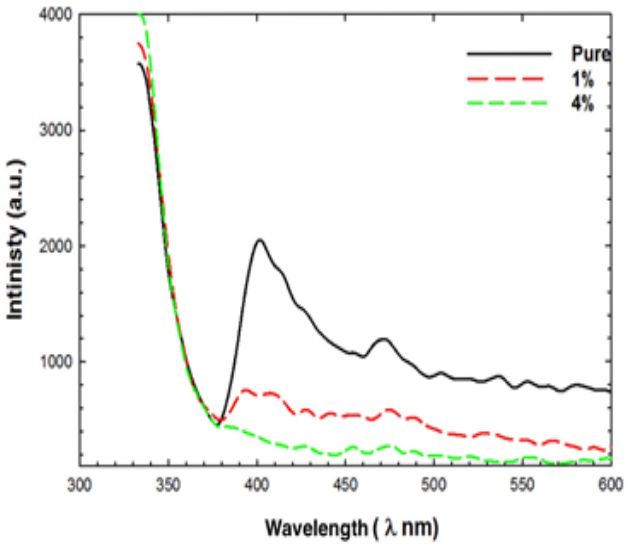

Fig. (4): The photoluminescence spectra of undoped (zinc oxide) and manganese doped zinc oxide at 1%, 4%

The intrinsic defect centers such as oxygen interstitials. Zn interstitials, Zn vacancies, or oxygen vacancies are correlated with the green luminescence. The commonly cited explanation is that, the radiative recombination of a photo-generated hole often originates from the green emission with an electron occupying the oxygen vacancy [19,20].

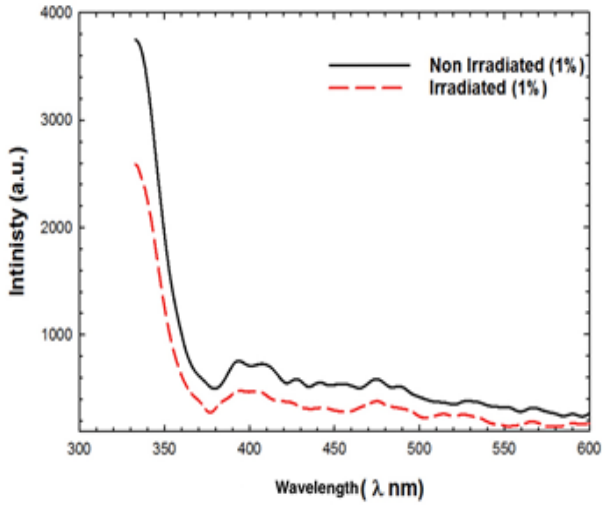

Fig. (5): The photoluminescence spectra at 1% of Mn-doped ZnO non-irradiated and gamma irradiated with 30 kGy with excitation wavelength of 323 nm

The transition, toward the ground state of the lowest excited state is arising from the tetrahedrally coordinated Mn^{2+} sites and it is clearly dependent on the green light emission [16]. Further concentration of Mn ions is in the tetrahedral sites recommends that, the intensity of green emission is of more contrast as compared to red emission.

The PL spectra at 1% of Mn doped ZnO of non-irradiated and gamma irradiated with 30 kGy with excitation wavelength of 323 nm is displayed in Fig. (5). The Mn^{2+} luminescence habits were studied by many authors [21-24]. It depends on the crystalline environment. By the formation of a weak crystal field, the tetrahedrally coordinated Mn^{2+} ion donates a green emission. After irradiation with gamma dose of 30 kGy, the PL peak intensity of Mn-doped ZnO decreased. The decrease in the PL intensity refers to the reduction of oxygen vacancies due to the indigent interface between ZnO/Mn.

4. CONCLUSION

By the co-precipitation method, the Mn-doped ZnO samples were synthesized successfully. No impurity phases, manganese metal or any extra peak of oxides and no signature impurity peaks were identified. It means that all samples are single phase. The intensity of the diffraction peaks corresponds to the hkl planes marked that all sintered samples have hexagonal (wurtzite) crystal structure.

The lattice parameters elevate with increasing Mn concentration in the doped ZnO. The crystallite average size reduces with raising the Mn percentage concentrations. The doping of various Mn percentages in ZnO may control the crystal size. However, the increase in the Mn concentration leads to increasing the volume of unit cell . This is possibly attributed to the increase in the lattice parameters. With raising Mn concentration, the atomic packing fraction (APF) increases, which indicates homogenous substitution of Mn ions in ZnO.

The influence of Mn on the Eg of the ZnO doped with Mn^{2+} ions of wurtzite structure in the tetrahedral sites of ZnO is confirmed using UV-Visible optical spectroscopy. Many reasons may contribute to the recorded reduction in the band gap during the rising in Mn content such as the appearance of defects such as oxygen vacancies.

In the photoluminescence spectra, ultraviolet emission is recorded concerning the undoped and Mn-doped ZnO nanoparticles. The shift in the photoluminescence emission peak of the doped nano-crystals in contrast with the photoluminescence emission of undoped nanocrystals is related to the shift in Eg. The reported results confirmed that the synthesized Mn doped ZnO nanostructures may be used in the prodution of an effective photocatalyst.

5. REFERENCES

[1] Iqbal, J.; Liu, X.; Majid, A.; Yu, R.: Synthesis and physical properties of Mn doped ZnO dilute magnetic semiconductor nanostructures. *Journal of Superconductivity and Novel Magnetism*, vol. 24, no. 1-2, pp. 699–704 (2011).

[2] Raval, H. D.; Gohil, J. M.: Nanotechnology in water treatment: an emerging trend. *International Journal of Nuclear Desalination*, vol. 4, no. 2, pp. 184–188, (2010).

[3] Tong Ling Tan; Chin Wei Lai; Sharifah Bee Abd Hamid. Tunable Band Gap Energy of Mn-Doped ZnO Nanoparticles Using the Coprecipitation Technique. Journal of Nanomaterials. Article ID 371720, 6 pages (2014).

[4] Wang, L. W.; Xu, Z.; Zhang, F. J.; Zhao, S. L; Lu, L. F.: Structure, optical, and magnetic properties of Mn-doped ZnO films prepared by sputtering," *International Journal of Minerals,Metallurgy and Materials*, vol. 17, no. 4, pp. 475–480 (2010).

[5] Yan, X. X.; Xu, G. Y.: Effect of sintering atmosphere on the electrical and optical properties of (ZnO)1-x(MnO2)x NTCR ceramics. *Physica B*, vol. 404, no. 16, pp. 2377–2381 (2009).

[6] VOICU, G.; OPREA, B.; VASILE, S.; RONESCU: Photoluminescence And Photocatalytic Activity Of Mn-Doped ZnO Nanoparticles, Vol. 8, No. 2, p. 667 – 675. (2013).

[7] LILA A. ALKHTABY, SHAHID HUSAIN, WASI KHAN, ALIM H. NAQVI, S.: Structural and Optical Properties of Mn Doped ZnO Nanoparticles. Asian Journal of Chemistry; Vol. 23, No. 12, 5605-5607 (2011).

[8] Sharma, R. K.; Sandeep Patel, R. K.; Pargaien. K. C.: Synthesis, characterization and properties of Mndoped ZnO nanocrystals. *Adv. Nat. Sci: Nanosci. Nanotechnol.* 3 035005. (2012).

[9] Mote, V. D.; Dargad, J. S.; Dole, B. N.: Effect of Mn Doping Concentration on Structural, Morphological and Optical Studies of ZnO Nano-particles. Nanoscience and Nanoengineering 1(2): 116-122, (2013).

[10] Volbers, N.; Zhou, H.; Knies, C.; Pfisterer, D.; Sann, J.; Hofmann, D. M.; Meyer, B. K.: Synthesis and characterization of ZnO:Co²⁺ nanoparticles. Applied Physics A: Materials Science & Processing 2007, 88 (1), 153-5 (2007).

[11] Li, L.; Wang, W.; Liu, H.; Liu, X.; Song, Q.; Ren, S.: First principles calculations of electronic band structure and optical properties of Cr-doped ZnO. The Journal of Physical Chemistry C, 113 (19), 8460-4 (2009)..

[12] Mott, N.F.; Davis, E.A.: Electronic Process in Non-Crystalline Materials, Clar- endon Press, Oxford (1979).

[13] Abdollahi, Y.; Abdullah, A. H.; Zainal, Z.; Yusof N. A. Synthesis and characterization of Manganese doped ZnO Nanoparticles" International Journal of Basic & Applied Sciences IJBAS-IJENS Vol: 11 No: 04, (2011).

[14] Lee, Y. R.; Ramdas, A.K.;.Aggarwal, R.L: Phys. Rev. B: Condens. Matter 38, 10600 (1988)..

[15] Abdel-Galil, A.; Balboul, M.R.; Sharaf, A.: Synthesis and characterization of Mn-doped ZnO diluted magnetic semiconductors. Physica B 477, 20–28 (2015).

[16] Sowri Babu, K; Srinath, P; Rajeswara Rao, N.; Venugopal Reddy,K.: Effect of Gamma Irradiation on Structural and Optical Properties of ZnO/Mesoporous Silica Nanocomposite. International Journal of Physical and Mathematical Sciences Vol:11, No:6, (2017).

[17] Morkoç, H; Özgür, Ü.; Zinc Oxide: Fundamentals, Materials and Device Tech- nology, WILEY-VCH Verlar Gmbh & Co. KGaA, Weinheim, p. 11 (2009).

[18] Jin B. J.; Bae S. H.; Lee S. Y; Im S.; Mater. Sci. Eng. B 71 301 (2000).

[19] Junnfeng Zhao; Zhida Han; Hongbin Lu,Xuhong Wang, Jianhuan Chen: J. Mater Sci:Mater Electron 22, 1361 (2011).

[20] Wang, Y.H.; Duan, W.J.; Wu, Z.L.; Zheng, D.; Zhou, X.W.; Zhou, B.Y.; Dai, L.J.; Wang, Y.S.: J.Lumin.132,1885 (2012).

[21] Husain,S.; Alkhtaby, L.A.; Giorgetti, E.; Zoppi, A.; Muniz, M.: J. Lumin. 145, 132 (2014)

[22] R.K Sharma,Sandeep Patel, K.C Pargaien, Adv. Nat. Sci.:Nanosci. Nanotechnol. 3, 035005 (2012).

[23] Bulyk, L.-I.; Vasylechko, L.; Mykhaylyk, V.; Tang, C.; Zhydachevskyy, Ya.; Hizhnyi, Y. A.; Nedilko, S. G.; Klyui, N. I.; Suchocki, A.: Mn2+ luminescence of Gd(Zn,Mg)B5O10 pentaborate under high pressure. Dalton Transactions Journal, Issue 40 (2020).

[24] Rebecca B. Wai, Namrata Ramesh, Clarice D. Aiello, Jonathan G. Raybin, Steven E. Zeltmann, Connor G. Bischak, Edward Barnard, Shaul Aloni, D. Frank Ogletree, Andrew M. Minor, and Naomi S. Ginsberg. Resolving Enhanced Mn2+ Luminescence near the Surface of CsPbCl3 with Time-Resolved Cathodoluminescence Imaging. J. Phys. Chem. Lett. 11, 7, 2624–2629 (2020).